Hybrid Energy Harvesting Cooperative Spectrum Sensing in Heterogeneous CRNs

Abdulkadir Celik, Ahmad Alsharoa, Ahmed E. Kamal
Department of Electrical and Computer Engineering,
Iowa State University (ISU), Ames, Iowa, United States,
Email: {akcelik, alsharoa, kamal}@iastate.edu

***Abstract*—*Energy Harvesting* and *Energy Efficient* (EEH) Cognitive Radio Networks (CRNs) is one of the key technologies to meet the next generation wireless network demands for high *energy and spectrum efficiency*. EEH-CRNs can enable self-sustaining green communications by reducing the energy cost and harvesting the ambient energy sources while capitalizing the idle spectrum simultaneously. In this paper, we first propose a hybrid EH-SU model to harvest energy from both renewable sources, e.g. solar, and ambient radio frequency signals. A general hybrid cooperative spectrum sensing (CSS) scheme is then considered with and without energy *half-duplex* (EHD) constraint which prevents SUs from charging and discharging the battery at the same time. As an alternative to common homogeneity assumption, we propose a heterogeneous EEH-CSS scheme to exploit heterogeneous sensing and reporting channel characteristics of SUs. After formulating the energy state evolution under stochastic energy arrivals, a convex myopic EEH-CSS policy optimization framework is then developed to jointly obtain the optimal harvesting ratio, sensing duration and detection threshold of each SU to maximize the total achievable throughput subject to *collision and energy-causality* constraints. Obtained results show that the proposed heterogeneous approach delivers $\%45$ and $\%230$ more throughput than the homogeneous one with and without EHD constraint, respectively. Furthermore, if the EHD constraint is mitigated, proposed heterogeneous approach provides $\%400$ and $\%240$ more throughput than the EHD constrained homogeneous and heterogeneous EHE-CSS schemes, respectively.**

I. Introduction

A. Motivation

To fulfill the ambitious demands of the next generation wireless communication networks, e.g. 1000 times heavier data traffic and 100 times less energy consumption per bit [1], researchers in both academy and industry focus on *energy and spectrum efficient* solutions. CRNs have already received a great attention from both communities to mitigate the inefficient fixed spectrum allocation policy with the novel idea of utilizing idle licensed spectrum in an opportunistic manner. However, a substantial portion of above demands has recently migrated to mobile wireless networks and devices with limited energy resources. Considering the fact that 30% of the energy expenditure of mobile devices is caused by wireless networking and computing modules [2], energy efficient (EE) CRNs play a vital role to provide portable devices with more spectrum for less energy consumption. Because approximately 2% of the worldwide CO_2 emissions is caused by the communications and information technologies [4], energy efficient policies are becoming more important to achieve green communication standards.

In this regard, communication community recently focuses on EH communications to obtain significant advantages over traditional grid-powered and non-rechargeable and/or battery-powered wireless devices [5]. By harvesting required energy from alternative natural resources such as solar, vibrational, thermoelectric, and radio frequency (RF) signals etc., EH cognitive radios (CRs) can achieve self-sustaining green communications. For a given amount of energy, conventional EE-CRNs aims to minimize the total sensing energy consumption subject to the fundamental *collision constraint* to prevent unlicensed users, a.k.a secondary users (SUs), from interfering with the licensed users, a.k.a primary users (PUs). In EH systems, on the other hand, energy needed for sensing and data transmission arrives intermittently and in random magnitudes of energy because of the random nature of EH sources. Then, the ultimate goal of EEH-CRNs would be, not only to minimize the over-all energy consumption, but to also maintain sensing and transmitting tasks under random and intermittent energy arrivals. Such a goal dictates an extra fundamental limit on the capacity of traditional CRNs: *energy-causality constraint* which states that the energy harvested by a time instant must be greater than or equal to the consumed energy until that time instant [6]. Furthermore, ultra-capacitors are preferred to store harvested energy due to their high power density, good recycling ability, and near perfect storing efficiency. Albeit these favorable features, ultra-capacitors are subject to *energy half-duplex* (EHD) constraint which prevents SUs from charging and discharging simultaneously. As a result, EHD constraint leads to a performance degradation in harvested energy amount and available time left for data transmission because SUs have to share the available time for harvesting, sensing, and transmitting [7].

B. Related Work

In his early work, Sultan considers a non-cooperative spectrum sensing where a single EH-SU tries to maximize the throughput while making decision on being either dormant or active to sense the primary channel (PC) based on a Markov decision process (MDP) [8]. In [9]–[11], authors investigate the effects of energy arrivals on spectrum sensing and access policies of a single EH-SU. In accordance with the energy arrival rate, they also define *energy-limited* and *spectrum-limited* regimes for a fixed sensing duration. Even though above works provide a valuable insight into the non-cooperative EH spectrum sensing, detection performance of a single SU is severely affected by channel impairments. As a remedy, *Cooperative spectrum sensing* (CSS) is a powerful solution to alleviate these by taking advantage of the spatial diversity of SUs to obtain higher confidence [12]. Moreover, [9]–[11] optimize the energy consumption of the SU by adjusting the detection threshold for a fixed sensing duration. However, joint optimization of sensing durations and detection thresholds of SUs is necessary in CSS.

Inspired by [13], Yin et al. studies the fundamental tradeoffs among harvesting, sensing, and transmission duration in CSS with the EHD constraint [14]. Based on homogeneous signal-to-noise-ratio (SNR) and perfect common control channel (CCC) assumption, they develop the theoretical basis of CSS under the EHD constraint. Likewise, for a homogeneous EH-CSS scenario where SUs harvest energy from RF signals, the optimal sensing probability and harvesting duration of each SU is obtained to maximize the throughput while satisfying the energy causality and PU collision constraints [15]. Similarly, authors of [16] consider a homogeneous CSS setting to find the optimum balance between average probability of global detection, probability of false alarm and probability of having an active SU to transmit with the available harvested energy. On the other hand, Ala et al. propose two strategies using which the individual needs are reflected on the final decision by means of adjusting the local detection thresholds [17]. Finally, a finite-horizon POMDP is considered to obtain the optimal cooperation among the SUs for sensing and access to maximize throughput with the available energy while satisfying the PU detection constraint [18]. CSS schemes in [14]-[18] use the 'OR' fusion rule which is mathematically more tractable but less energy efficient [19]. Except [17], [14]-[18] do not consider the imperfection of CCC. However, the total energy consumption of CSS increases with the increasing reporting error until an error wall after which reliable spectrum sensing is not feasible [20]. In particular, heterogeneity of the sensing and reporting quality of cooperating SUs is another complexity which is not considered in these works.

C. Main Contributions and Novelty

The main contributions of this paper can be summarized as:

1) In this paper, we propose a *hybrid* EH-CSS scheme where SUs can harvest energy from both renewable sources, e.g. solar, and ambient RF signals. In order to mitigate the EHD constraint, Luo et al. proposed the simple and yet novel idea of using two different ultra-capacitors to charge and discharge at the same time [7]. Accordingly, we generalize their model to investigate the performance of a hybrid EH-CSS with and without the EHD constraint.
2) Under the common assumption of homogeneous sensing and reporting channels (e.g., identical SNRs, reporting errors etc.), optimal sensing durations of all SUs will be the same. In this case, *Binomially* distributed K-out-of-N rule is extensively employed to conclude a global decision by enforcing SUs to have identical detection and false alarm reports at fusion center (FC). In practical cases where SUs have heterogeneous sensing and reporting channel qualities, however, enforcing SUs to have identical local reports at the FC will cause more energy consumption since SUs with relatively low SNRs are required to sense longer. As a result, Binomial K-out-of-N is also throughput inefficient under heterogeneous scenarios since the FC must wait for the slowest SU. This is mainly because of the fact that the FC will not diffuse back the final decision and access policy until it collects all reports. Therefore, to capitalize from the sensing and reporting quality diversity of SUs, we propose a heterogeneous CSS framework by employing a *Poisson-Binomial (P-Binomial)* based K-out-of-N rule where SUs with different sensing and reporting qualities are allowed to have different reported detection performances.
3) After demonstrating the differences in the timeslotted operation of SUs due to the heterogeneity, we develop the energy state evolution for EH-CSS with and without EHD constraint. Based on SUs' energy states, a convex myopic policy optimization framework is developed to find the optimal EH policy to jointly obtain the optimal harvesting ratio, sensing duration and detection threshold of each SU which maximizes the sum of the achievable throughput of SUs subject to *collision and energy-causality* constraints.
4) The performance of CSS with/without EHD constraint and under homogeneity/heterogeneity is numerically analyzed. Obtained results clearly show that the proposed heterogeneous CSS scheme without EHD constraint gives the best performance in terms of sensing energy cost reduction, achievable throughput maximization and harvested energy accumulation.

D. Paper Organization

The rest of this paper is organized as follows: Section-II models the hybrid EH based on stochastic energy arrivals. Section-III, introduces the proposed CSS scheme. After that, Section-IV characterizes the energy state evolution of each SU and formulates the convex myopic policy optimization. Numerical results are presented in Section-V. Finally, we conclude the paper in Section-VI with a few remarks.

II. System Model

We consider a CRN comprised of a single PC and M time synchronous and self-powered EH-SUs. The PU works in a time slotted fashion such that the PC is either in a busy or idle state for a given timeslot. Similarly, SUs also cooperatively operate in timeslots of T seconds to harvest, sense and utilize the PC. To facilitate the analysis in this paper, we assume that SUs always have data to transmit and demands for as higher achievable throughput if available. We model the stochastic energy arrival rate of SU m as a random variable Λ_m in $[Joule/s]$ which follows a general distribution function with mean λ_m and variance σ_m^2. For example, Λ_m can be interpreted as the received amount of energy per time unit with respect to received luminous intensity of a solar panel in a particular direction per unit solid angle. The energy arrival rate within a timeslot t, λ_m^t, is assumed to be time invariant.

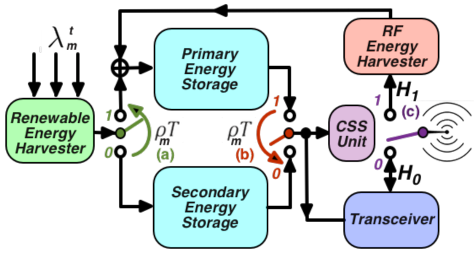

Figure 1: Generalized Hybrid EH-SU Model.

Based on the idea in [7], generalized hybrid EH-SU model is shown in Figure 1 where the switch (a) splits the renewable energy arrivals in time without interrupting the sensing-reporting-transmitting of the SU; $\rho_m T$ and $(1-\rho_m)T$ durations are allocated for storing the harvested energy on the PES and the SES, respectively. The switch (b) works in opposite direction of the switch (a) to power the SU, i.e., while the PES (SES) collects energy arrivals the SES (PES) powers the SU. Assuming negligible time and energy loss due to switching, the SU will be able to harvest energy for the whole timeslot while powering the SU uninterruptedly. Right after execution of the local sensing, reporting and receiving the global decision, CSS unit toggles the switch (c) to position 0 in the case of PU absence to transmit secondary data, otherwise it toggles the purple switch to position 1 to harvest RF energy from the busy PC. To put distinction between each other, we refer to CSS schemes with and without EHD constraint as energy half-duplex system (EHS) and energy full-duplex system (EFS), respectively.

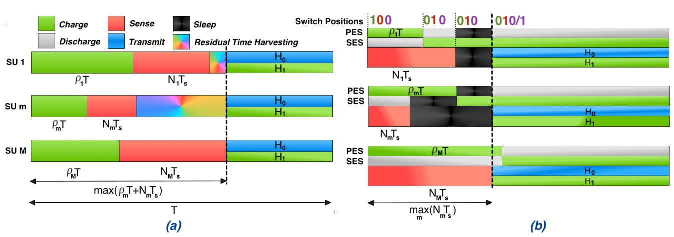

Figure 2: Time-slot Representation of SUs with (a) EHS and (b) EFS.

A. Time-slotted Operation for Energy Half-Duplex (EHD) CSS

EHS can be obtained as a specific case of the generalized model in Figure 1 by eliminating the SES and keeping the switch (b) in position 1 all the time. In the EHS, as shown in Figure 2.a, SU m harvest renewable energy for $\rho_m T$ seconds, then use the stored available energy from the previous timeslot along with the harvested energy in the current timeslot to complete CSS tasks. Right after the sensing duration, SUs except for the slowest one keep harvesting energy until they receive a global decision feedback from the FC, which is shown as a multicolor portion of the timeslot in 2.a. Based on the decision, the residual time will be used for the secondary data transmission by toggling the switch (c) to position 0 if the PC is idle, otherwise it will be toggled to position 1 for RF-EH until the beginning of next timeslot.

B. Time-slotted Operation for Energy Full-Duplex (EFD) CSS

The timeslotted operation of the EFS is demonstrated in Figure 2.b where the positions of switches have also been shown in zeros and ones for the first SU to provide readers with more insight into operation of the generalized model. By using the SES, the SUs are now able to harvest energy for the entire timeslot while also using the entire timeslot for sensing and transmitting/RF harvesting. As mentioned earlier, the different sensing duration of SUs problem still applies and SUs put themselves into *sleep mode* to save energy until they receive a decision from the FC. Threfore, EFS intuitively provides : 1) More harvested energy, and 2) more throughput, since the timeslot is not shared between harvesting and sensing+transmission. We also note that both EHS and EFS models may further be simplified for SUs which are solely empowered by RF-EH by eliminating the renewable energy harvester and replacing the RF energy harvester with it.

III. Cooperative Spectrum Sensing

Since the focus of this paper is the EH aspects of CRNs, a generic sensing method like *energy detection* is adequate for local detectors. Energy detectors (EDs) have been extensively exploited as the ubiquitous sensing technique in the literature due to its simplicity, compatibility with any signal type, and low computational and implementation complexity [21]. We denote the binomial hypothesis for the idle and busy state of the PC as $\mathcal{H}_0$ and $\mathcal{H}_1$, respectively. Based on long time observations, the secondary network is aware of the *apriori* probability of idle and busy state of the PC which are denoted as $\pi_0 = \mathcal{P}[\mathcal{H}_0]$ and $\pi_1 = \mathcal{P}[\mathcal{H}_1]$, respectively. To detect primary signals, ED of SU m measure the received signal energy for a number of samples N_m and compares it with a threshold ε_m to decide on the PU activity status. For a large enough number of samples ($N_m \geq 30$) and normalized noise variance, probability of false alarm, P_m^f, and probability of detection, P_m^d, are respectively given by [13]

$$P_m^f(N_m, \varepsilon_m) = \mathcal{Q}\left[(\varepsilon_m - 1)\sqrt{N_m}\right] \tag{1}$$

$$P_m^d(N_m, \varepsilon_m) = \mathcal{Q}\left[(\varepsilon_m - \gamma_m - 1)\sqrt{\frac{N_m}{2\gamma_m + 1}}\right] \tag{2}$$

where γ_m and $\mathcal{Q}(\cdot)$ denote the SNR of SU$_m$ and the Q-function, respectively. After the local sensing process, SUs send their hard results, u_m, to the FC over a binary symmetric CCC. Denoting the reporting error probability as $P_b = \mathcal{P}[\tilde{u}_m = 1 | u_m = 0] = \mathcal{P}[\tilde{u}_m = 0 | u_m = 1]$ where $\tilde{u}_m$ is the hard decision received by the FC, the local false alarm and

EHS	Global Decision: $\mathcal{H}_0$	Global Decision: $\mathcal{H}_1$
π_0	$\min\left(S_m^h, S_m^{t-1}+\Delta_m^h-E_m^{tx}\right)$	$\min\left(S_m^h,\ S_m^{t-1}+\Delta_m^h+\lambda_m^t\left(T-\Gamma^h\right)\right)$
π_1	$\min\left(S_m^h, S_m^{t-1}+\Delta_m^h-E_m^{tx}\right)$	$\min\left(S_m^h,\ S_m^{t-1}+\Delta_m^h+\lambda_m^t\left(T-\Gamma^h\right)+\Delta_m^{rf,h}\right)$
EFS	**Global Decision: $\mathcal{H}_0$**	**Global Decision: $\mathcal{H}_1$**
π_0	$\min\left(S_m^f, S_m^{t-1}+\Upsilon_m-N_mE_s-E_m^{tx}\right)$	$\min\left(S_m^f, S_m^{t-1}+\Upsilon_m-N_mE_s\right)$
π_1	$\min\left(S_m^f, S_m^{t-1}+\Upsilon_m-N_mE_s-E_m^{tx}\right)$	$\min\left(S_m^f, S_m^{t-1}+\Upsilon_m-N_mE_s+\Delta_m^{rf,f}\right)$

Table I: Energy States at the beginning of timeslot t, S_m^t.

detection probabilities received at the FC side are given by

$$\begin{aligned}\tilde{P}_m^f &= \mathcal{P}\left[\tilde{u}_m=1|u_m=0\right]\mathcal{P}\left[u_m=0|\mathcal{H}_0\right]\\ &\quad+\mathcal{P}\left[\tilde{u}_m=1|u_m=1\right]\mathcal{P}\left[u_m=1|\mathcal{H}_0\right]\\ &= P_b\left(1-P_m^f\right)+\left(1-P_b\right)P_m^f \qquad (3)\\ \tilde{P}_m^d &= \mathcal{P}\left[\tilde{u}_m=1|u_m=0\right]\mathcal{P}\left[u_m=0|\mathcal{H}_1\right]\\ &\quad+\mathcal{P}\left[\tilde{u}_m=1|u_m=1\right]\mathcal{P}\left[u_m=1|\mathcal{H}_1\right]\\ &= P_b\left(1-P_m^d\right)+\left(1-P_b\right)P_m^d \qquad (4)\end{aligned}$$

The FC collects $\tilde{u}_m$'s and makes the global decision using the following test

$$\mathcal{K}=\sum_{m=1}^{M}\tilde{u}_m \underset{\mathcal{H}_0}{\overset{\mathcal{H}_1}{\gtrless}} \kappa \qquad (5)$$

which follows the *P-Binomial* distribution (Under the common homogeneity assumption, $\mathcal{K}$ follows *Binomial* distributions as a special case by enforcing $\tilde{P}_m^f=\tilde{P}^f$, $\tilde{P}_m^d=\tilde{P}^d$, $\forall m$). Using equations (3) and (4) in P-Binomial distribution, the FC obtains the global false alarm and detection probabilities by fusing the local reports as follows [22]

$$\begin{aligned}Q_f &= \mathcal{P}\left[\mathcal{K}\geq\kappa \mid \mathcal{H}_0\right]\\ &= \sum_{i=\kappa}^{M}\sum_{A\in F_i}\prod_{m\in A}\tilde{P}_m^f\prod_{m\in A^c}\left(1-\tilde{P}_m^f\right) \qquad (6)\\ Q_d &= \mathcal{P}\left[\mathcal{K}\geq\kappa \mid \mathcal{H}_1\right]\\ &= \sum_{i=\kappa}^{M}\sum_{A\in F_i}\prod_{m\in A}\tilde{P}_m^d\prod_{m\in A^c}\left(1-\tilde{P}_m^d\right) \qquad (7)\end{aligned}$$

where F_i is the set of all subsets of i integers that can be selected from $\{1,2,3,\ldots,M\}$. Since F_i has $\binom{M}{i}$ elements, using an efficient method to calculate Eq. (6) and (7) is very important, especially when M is very large. For this purpose, probability mass function (pmf) and cumulative distribution function of *P-Binomial* random variables can be expeditiously calculated in order of $\mathcal{O}(M\log_2 M)$ from polynomial coefficients of the probability generating function of $\mathcal{K}$ [23].

IV. Energy State Evolution and Myopic Policy Optimization

In EH-CSS, energy states of SUs evolve over time such that energy state in the next timeslot depends on the energy state and action taken (i.e., duration of harvesting, sensing, and transmitting) in the current timeslot. For EHS, there is a single battery with Let $\eta_m^1\in[0,1]$ ($\eta_m^2\in[0,1]$) and S_m^1 (S_m^2) denote the storing efficiency and storage capacity of the SES (PES), respectively. For the sake of comparison, we assume that EHS and EFS have exactly the same total battery capacity, i.e. $S_m^h=S_m^f=S_m^1+S_m^2$ where superscripts h and f refer to EHS and EFS, respectively. At the beginning of the each timeslot t, SU is aware of available energy levels in the PES and SES. RF energy harvesting rate is given by

$$\lambda_m^{rf,t}=P(\delta_m^t)^{-\alpha}\eta_m^{rf}\ \mathbb{I}\left[P(\delta_m^t)^{-\alpha}>\bar{P}\right]\ [Watt] \qquad (8)$$

where P denotes the transmission power of the RF source, $(\delta_m^t)^{-\alpha}$ is the path loss over the distance δ_m^t with the corresponding path loss exponent α, η_m^{rf} denotes the efficiency of RF-to-DC converter circuit, and $\mathbb{I}\left[P(\delta_m^t)^{-\alpha}>\bar{P}\right]$ is the indicator function to impose RF-to-DC circuitry sensitivity on the received RF power such that there is no gain if the received power is less than the sensitivity threshold, $\bar{P}$.

We define the maximum time spent for harvesting+sensing for EHS/EFS in (9)/(10), the net gained energy until the global decision feedback for EHS/EFS in (11)/(12), harvested energy from RF source for EHS/EFS in (13)/(14), and the total harvested energy from renewable source for EFS in (15) as follows

$$\begin{aligned}\Gamma^h &= \max\left(\rho_mT+N_mT_s\right) &(9)\\ \Gamma^f &= \max\left(N_mT_s\right) &(10)\\ \Delta_m^h &= \lambda_m^t\eta_m\left(\Gamma^h-N_mT_s\right)-N_mE_s &(11)\\ \Delta_m^f &= \lambda_m^t\left[\eta_m^1\rho_mT+\eta_m^2[\Gamma-\rho_mT]^+\right]-N_mE_s &(12)\\ \Delta_m^{rf,h} &= \lambda_m^{rf,t}\left(T-\Gamma^h\right) &(13)\\ \Delta_m^{rf,f} &= \lambda_m^{rf,t}\left(T-\Gamma^f\right) &(14)\\ \Upsilon_m &= \lambda_m^t\left[\eta_m^1\rho_m+\eta_m^2\left(1-\rho_m\right)\right]T &(15)\end{aligned}$$

where T_s is the sensing duration per sample, E_s is the sensing energy expenditure per sample, $[x]^+\triangleq\max(0,x)$, $E_m^{tx}=\min\left(E_m, S_m^{t-1}+\Delta_m\right)$ is the transmission energy where $0\leq E_m\leq S_m$ is the allocated transmission energy for SU_m. By setting $E_m=S_m^{t-1}+\Delta_m$, SUs exhaust all available residual energy for secondary data transmission, otherwise residual energy of SUs for the next timeslot will be S_m^t which is shown for all four cases in Table I. For normalized powers, the total expected achievable throughput of the secondary network is then given by

$$\begin{aligned}R_h &= \pi_0\left(1-Q_f\right)R_{00}^h\\ &= \pi_0\left(1-Q_f\right)\sum_m\frac{T-\Gamma^h}{T}\log_2\left[1+\frac{E_m^{tx}}{T-\Gamma^h}\right] \qquad (16)\end{aligned}$$

$$R_f = \pi_0 (1-Q_f) R_{00}^f = \pi_0 (1-Q_f) \sum_m \frac{T-\Gamma^f}{T} \log_2 \left[1 + \frac{E_m^{tx}}{T-\Gamma^f}\right] \quad (17)$$

where E_m^{tx} is the transmission energy of the SU m. Based on energy state evolution of SUs, an optimal design for EH and sensing strategy can be formulated as an MDP with an uncountable and continuous state and action space. Hence, we will consider a myopic policy which only focuses on current timeslot by ignoring its effects on future rewards, thus, SUs will decide to sense and transmit whenever they satisfy the energy causality constraint. It has been shown that a myopic policy is very close to the optimal policy with greatly reduced computational cost [24]. Accordingly, we can formulate the problem of maximizing the achievable throughput for EHS as in $\mathbf{P_1}$ where we take the logarithm of (16) to put the objective in a convex form. $\mathbf{P_1}$ is a convex mixed-integer non-linear programming (MINLP) problem whose mixed-integer nature is due to the variables N_m and κ. It is a practical approach to relax the problem by unintegerizing N_m. After obtaining the optimal reel valued solution, one can obtain the closest upper integer value, which does not negatively effect the system performance since $N_m >> 1$ and $T_s,\ E_s << 1$. For the rest of the paper, we will employ the majority voting rule, $\kappa = \lceil M/2 \rceil$ where $\lceil \cdot \rceil$ denotes the ceiling operation, which has already been shown to be the optimal voting rule for required minimum SNR (i.e. required minimum sensing energy cost) of CSS [20]. Therefore, the following convexity analysis is based on the unintegerization of N_m for $\kappa = \lceil M/2 \rceil$.

$$\begin{aligned}
\mathbf{P_1}: \max_{\substack{\rho_m, N_m \\ \varepsilon_m,\ \forall m}} \quad & \log_2(\pi_0) + \log_2(1-Q_f) + \log_2\left(R_{00}^h\right) \\
1: \quad \text{s.t.} \quad & \log_2\left(\bar{Q}_d\right) \le \log_2(Q_d) \\
2: \quad & P_m^f \le 0.5,\ \forall m \\
3: \quad & 0.5 \le P_m^d,\ \forall m \\
4: \quad & 0 \le T - \Gamma^h \\
5: \quad & 0 \le S_m^{t-1} + \Delta_m^h,\ \forall m \\
6: \quad & 0 \le S_m^{t-1} + \lambda_m^t \eta_m \rho_m T \le S_m^h,\ \forall m \\
7: \quad & 30 \le N_m \le T/T_s,\ \forall m \\
8: \quad & k \in \mathbb{N}^+,\ N_m \in \mathbb{R}^+,\ \varepsilon \in \mathbb{R},\ \forall m
\end{aligned}$$

The first term of the objective function is a constant and out of the consideration. The second term is a concave function since Q_f (Q_d) are log-concave functions of $\tilde{P}_m^f$ ($\tilde{P}_m^d$) in both Binomial and P-Binomial distribution cases [19]. It is also non-decreasing in $\tilde{P}_m^f$ ($\tilde{P}_m^d$) since Q_f (Q_d) intuitively increases as SUs report with more confidence. Constraints in line 2 (line 3) is required to ensure the convexity (concavity) of $P_m^f \le 0.5$ ($P_m^d \ge 0.5$) since $\mathcal{Q}(\cdot) \le 0.5$ ($\mathcal{Q}(\cdot) \ge 0.5$) is a convex (concave) function. Indeed, constraining local detection probabilities to be higher than 0.5 and false alarm probabilities to be lower than 0.5 do not contradict practical cases of interests. $P_m^f \le 0.5$ ($P_m^d \ge 0.5$) also ensures the the convexity (concavity) of $\tilde{P}_m^f$ ($\tilde{P}_m^d$) since non-negative weighted summation preserves the convexity (concavity). Furthermore, exploiting the convex composition mechanics [25], the concavity of the $\log(1-Q_f)$ and the first constraint, $\log(Q_d) > \log(\bar{Q}_d)$, can be proven as in [19].

The last term in the objective is the logarithm of R_{00}^h which is a function of Γ^h in (9). Γ^h is a piece-wise maximum of functions $g_m(\rho_m, N_m) = \rho_m T + N_m T_s$ which is a linear function of (ρ_m, N_m) and constant for $(\rho_n, N_n),\ \forall n \neq m \in [1, M]$. Since piece-wise maximization preserves the convexity and $g_m(\rho_m, N_m), \forall m$ is linear, Γ^h is a convex function of $(\rho_m, N_m),\ \forall m$, which is again followed from the convex composition rules. On the other hand, since $\log(1+x)$ is concave and monotonically non-decreasing for non-negative x and perspective operation preserves concavity [25], the inner part of the last term can be considered as the perspective function of Γ^h. Thus, the last term of the objective is also concave following from the convex composition rules. Constraint 4, $\Gamma^h \le T$, defines the upper-bound of the maximum harvesting+sensing time as the timeslot duration. Constraint 5 enforces the system to have enough storage to execute the sensing operation for $N_m E_s$ amount of energy. Constraint 6 limits the harvesting rate since harvesting and storing energy up to a fully charged battery will not provide any additional energy. In constraint 7, N_m is lower-bounded to evoke the central limit theorem and upper-bounded to maximum permissible number of samples within a timeslot duration. For EFS, $\mathbf{P_1}$ can be modified to become $\mathbf{P_2}$ as follows:

$$\begin{aligned}
\mathbf{P_2}: \max_{N_m, \varepsilon_m,\ \forall m} \quad & \log_2(\pi_0) + \log_2(1-Q_f) + \log_2\left(R_{00}^f\right) \\
1: \quad \text{s.t.} \quad & \log_2\left(\bar{Q}_d\right) \le \log_2(Q_d) \\
2: \quad & 0.5 \le P_m^d,\ \forall m \\
3: \quad & P_m^f \le 0.5,\ \forall m \\
4: \quad & 0 \le T - \Gamma^f \\
5: \quad & 0 \le S_m^{1,t-1} + S_m^{2,t-1} + \Delta_m,\ \forall m \\
6: \quad & 0 \le S_m^{1,t-1} + \lambda_m^t \eta_m^1 \rho_m T \le S_m^1,\ \forall m \\
7: \quad & 0 \le S_m^{2,t-1} + \lambda_m^t \eta_m^2 (1-\rho_m) T \le S_m^2,\ \forall m \\
8: \quad & 30 \le N_m \le T/T_s,\ \forall m \\
9: \quad & k \in \mathbb{N}^+,\ N_m \in \mathbb{R}^+,\ \varepsilon \in \mathbb{R},\ \forall m
\end{aligned}$$

where constraints 5, 6 and 7 is adapted for EFS to apply the same reasoning given above. Even though the convexity analysis of $\mathbf{P_2}$ follows the same spirit of $\mathbf{P_1}$, it is worth indicating that the objective function of $\mathbf{P_2}$ is free of ρ_m. Unlike in EHS, this is because of the EFS feature that the entire timeslot is accessible for both harvesting and sensing + transmitting. SUs can spend the harvested energy in the beginning of a timeslot within the same timeslot, which requires joint optimization of all variables. Hence, if we allow SUs to expend only the residual energy from the previous timeslot, variables ρ_m and $(N_m,\ \varepsilon_m,\ \kappa)$ can be separated inherently. Such a policy can be formulated as

$$
\begin{aligned}
\mathbf{P_3}: \max_{\rho_m,\, \forall m} \quad & \Upsilon_m^1 = \lambda_m^t \left[\eta_m^1 \rho_m + \eta_m^2 (1-\rho_m)\right] T \\
1: \quad \text{s.t.} \quad & 0 \le S_m^{1,t-1} + \lambda_m^t \eta_m^1 \rho_m T \le S_m^1, \ \forall m \\
2: \quad & 0 \le S_m^{2,t-1} + \lambda_m^t \eta_m^2 (1-\rho_m) T \le S_m^2, \ \forall m
\end{aligned}
$$

where the objective is the total harvested energy during the entire timeslot and harvesting ratios are limited to the PES and SES capacity in lines 1 and 2, respectively. So that, once one of them is fully charged, we will switch to other in order to avoid wasting the energy arrivals. $\mathbf{P_3}$ can equivalently be written as

$$
\begin{aligned}
&\mathbf{P_4}: \max_{\rho_m} \ \rho_m \lambda_m^t \left(\eta_m^1 - \eta_m^2\right) T \\
&1: \quad \text{s.t.} \ \max\left(0, -\frac{S_m^{1,t-1}}{\lambda_m^t \eta_m^1 T}, 1 - \frac{S_m^2 - S_m^{2,t-1}}{\lambda_m^t \eta_m^2 T}\right) \le \\
&\qquad \rho_m \le \min\left(1, \frac{S_m^1 - S_m^{1,t-1}}{\lambda_m^t \eta_m^1 T}, 1 + \frac{S_m^{2,t-1}}{\lambda_m^t \eta_m^2 T}\right)
\end{aligned}
$$

Based on $\mathbf{P_4}$, finding the optimal harvesting policy of EFS is trivial and can be analyzed in three different cases:

1) $\eta_m^1 = \eta_m^2$: Any ρ_m within the feasible region is optimal.
2) $\eta_m^1 > \eta_m^2$: Optimal ρ_m is attained at the upper bound.
3) $\eta_m^1 < \eta_m^2$: Optimal ρ_m is attained at the lower bound.

Please note that the optimal harvesting ratio is independent from the storage capacities, S_m^1 and S_m^2.

V. Results and Analysis

To have identical total storage capacity and storing efficiency to establish a fair comparison between EHS and EFS, we deliberately enforce them to gave identical storage efficiency and total capacity. We assume that energy arrival intensity follows Gamma distribution with shape and scale parameters k and θ, respectively. To clearly show the impacts of heterogeneity, we consider cooperation of 5 SUs with -5, -10, -15, -20, -25 SNRs in dB. Unless it is explicitly stated otherwise, we employ the parameters given in Table II.

Par.	Value	Par.	Value	Par.	Value	Par.	Value
S_m^h, S_m^f	30 J	S_m^1	15 J	S_m^2	15 J	k, θ	0.75
η_m	0.99	η_m^1	0.99	η_m^2	0.99	η_m^{rf}	0.6
W_m	1 MHz	T	1 s	T_s	1 μs	π_0	0.4, 0.8
$\bar{Q}_d$	0.99	E_m^{tx}	4 J	E_s	1 μJ	α	2

Table II: Table of Parameters

For an EHS with an empty storage, Figure 3 compares the optimal values of traditional homogeneous (Binomial) and proposed heterogeneous (P-Binomial) CSS for $\lambda_m = 1 \ \forall m$, $\kappa = \lceil M/2 \rceil$, and $\bar{Q}_d = 0.99$. As can be seen in subplots (a) and (c), the SU with the lowest SNR has to expend its all harvested energy to sense for a long duration in order to achieve 0.9 (0.1) local P_d (P_f) to ensure $\bar{Q}_d = 0.99$ under the homogeneity assumption. As a result, the slowest SU does not leave time for channel utilization which yields zero throughput even if other SUs harvested energy for transmission. In the heterogeneous case, on the other

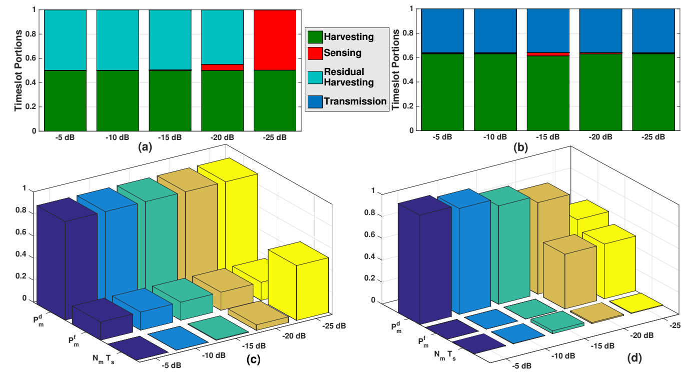

Figure 3: Comparison of homogeneous and heterogeneous cases: Optimal timeslot portions for (a) homogeneous and (b) heterogeneous; P_m^d, P_m^f, and sensing duration for (a) homogeneous and (b) heterogeneous.

hand, while SUs with relatively low SNRs are relaxed to have $P_m^d \simeq P_m^f \simeq 0.5$, SUs with relatively high SNRs are enforced to have nearly perfect local detection performances, $P_m^d \simeq P_m^f \simeq 1$ as shown in subplots (b) and (d). Therefore, by exploiting the SNR diversity of SUs, proposed approach yields a decreased sensing time (thus, energy) and increased time availability for harvesting and transmission. For 50 timeslots and 1000 different network scenarios, averaged results show that the proposed heterogeneous CSS gives $\%45$ and $\%230$ more throughput in EHS and EFS CSS schemes, respectively.

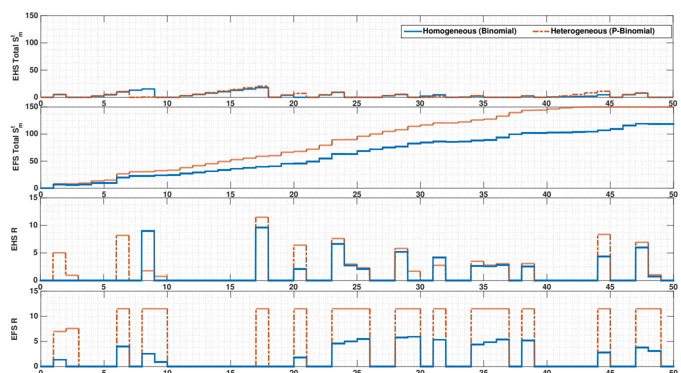

Figure 4: Horizontal energy levels and throughput for $\pi_0 = 0.4$.

Figure 4 demonstrates the above discussion for a finite horizon of size 50 where apriori probability of being idle for the channel is $\pi_0 = 0.4$. Top two plot shows the total storage of SUs, $\sum_m S_m^t$, at the beginning of the timeslots and bottom two plots show the achieved total throughput corresponding to the actual channel state. Since the PC is mostly busy, EFS accumulate energy due to the lack of chance to spend it for transmission. The stored energy difference between homogeneous and heterogeneous cases is caused from the energy inefficiency of homogeneity assumption as in Figure 3.(c). On the other hand, EHS cannot store energy like EFS since the available time is shared for harvesting, sensing and transmitting as in Figure 3.(a). In terms of the throughput, heterogeneous EHS has superior performance than the homogeneous one. For EFS, both homogeneous and heterogeneous approach have a better performance than the EHS. Among all combinations, it can be seen that the combining the EFS with the proposed heterogeneous CSS scheme gives the best solution.

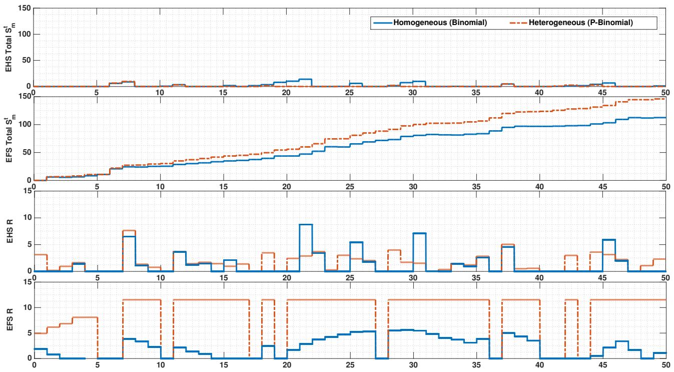

Figure 5: Horizontal energy levels and throughput for $\pi_0 = 0.8$.

	Hom. EHS	Het. EHS	Hom. EFS	Het. EFS
Hom. EHS	%0	%45	%55	%400
Het. EHS	-%35	%0	%5	%240

Table III: Performance enhancement of proposed methods.

Similar observations can be made for Figure 5 where the apriori probability of being idle for the channel is $\pi - 0 = 0.8$. In this case, the PU is mostly absent and SUs take advantage of this by utilizing the channel instead of not transmitting and saving the harvested energy. It is worth noting that if the energy arrival intensity increases the slope of the energy accumulation will also increase, or vice versa. Unlike Figure 4, the throughput difference between homogeneous and heterogeneous case of EFS is more significant. For 50 timeslots and 1000 different network scenarios, Table III shows the averaged throughput increase of proposed methods with respect to homogeneous and heterogeneous EHS performance.

VI. Conclusions

In this paper, we considered a hybrid generalized SU model, which can harvest energy from both renewable sources and ambient RF signals, to investigate the performance of EHE-CSS schemes with and without EHD constraints under the heterogeneous sensing and reporting channel characteristics of SUs. Unlike the traditional homogeneity assumption, a novel heterogeneous EHE-CSS scheme is proposed to capitalize the heterogeneous sensing and reporting channel diversity of SUs. Numerical results show that the proposed heterogeneous approach delivers $\%45$ and $\%230$ more throughput than the homogeneous one with and without EHD constraint, respectively. If the EHD constraint is mitigated, proposed heterogeneous approach also provides $\%400$ and $\%240$ more throughput than the EHD constrained homogeneous and heterogeneous EHE-CSS schemes, respectively.

References

[1] J. Andrews *et al.*, "What will 5g be?" *IEEE Journal on Selected Areas in Communications*, vol. 32, no. 6, pp. 1065 –1082, July 2014.

[2] S. Pollin *et al.*, "Meera: Cross-layer methodology for energy efficient resource allocation in wireless networks," *IEEE Transactions on Wireless Communications*, vol. 7, no. 1, pp. 98–109, 2008.

[3] G. Gur and F. Alagoz, "Green wireless communications via cognitive dimension: an overview," *IEEE Network*, vol. 25, no. 2, pp. 50–56, 2011.

[4] M. Webb *et al.*, "Smart 2020: Enabling the low carbon economy in the information age," *The Climate Group. London*, vol. 1, no. 1, pp. 1–1, 2008.

[5] V. Raghunathan *et al.*, "Emerging techniques for long lived wireless sensor networks," *IEEE Communications Magazine*, vol. 44, no. 4, pp. 108–114, Apr. 2006.

[6] O. Ozel *et al.*, "Fundamental limits of energy harvesting communications," *IEEE Communications Magazine*, vol. 53, no. 4, pp. 126–132, 2015.

[7] S. Luo *et al.*, "Optimal save-then-transmit protocol for energy harvesting wireless transmitters," *IEEE Transactions on Wireless Communications*, vol. 12, no. 3, pp. 1196–1207, Mar. 2013.

[8] A. Sultan, "Sensing and transmit energy optimization for an energy harvesting cognitive radio," *IEEE Wireless Communications Letters*, vol. 1, no. 5, pp. 500–503, 2012.

[9] S. Park *et al.*, "Cognitive radio networks with energy harvesting," *IEEE Transactions on Wireless Communications*, vol. 12, no. 3, pp. 1386–1397, 2013.

[10] S. Park and D. Hong, "Optimal spectrum access for energy harvesting cognitive radio networks," *IEEE Transactions on Wireless Communications*, vol. 12, no. 12, pp. 6166–6179, 2013.

[11] ——, "Achievable throughput of energy harvesting cognitive radio networks," *IEEE Transactions on Wireless Communications*, vol. 13, no. 2, pp. 1010–1022, 2014.

[12] I. F. Akyildiz *et al.*, "Cooperative spectrum sensing in cognitive radio networks: A survey," *Physical communication*, vol. 4, no. 1, pp. 40–62, 2011.

[13] E. C. Y. Peh *et al.*, "Optimization of cooperative sensing in cognitive radio networks: A sensing-throughput tradeoff view," *IEEE Transactions on Vehicular Technology*, vol. 58, no. 9, pp. 5294–5299, Nov. 2009.

[14] S. Yin *et al.*, "Achievable throughput optimization in energy harvesting cognitive radio systems," *IEEE JSAC*, vol. 33, no. 3, pp. 407–422, Mar. 2015.

[15] H. Liu *et al.*, "Optimal cooperative spectrum sensing strategy in cognitive radio networks exploiting rf-energy harvesting," in *proc. IEEE Intl. Conf. Wireless Communications & Signal Processing (WCSP)*, 2015, pp. 1–5.

[16] K. Li *et al.*, "Energy-harvesting cognitive radio systems cooperating for spectrum sensing and utilization," in *proc. IEEE GLOBECOM*, 2015.

[17] A. Alkheir *et al.*, "Cooperative spectrum sensing for rf-energy harvesting cognitive radio networks," in *proc. IEEE ICC*, 2015, pp. 7492–7497.

[18] P. Pratibha, K. H. Li, and K. C. Teh, "Dynamic cooperative sensing-access policy for energy-harvesting cognitive radio systems," *IEEE Transactions on Vehicular Technology*, 2015.

[19] A. Celik and A. E. Kamal, "Multi-objective clustering optimization for multi-channel cooperative spectrum sensing in heterogeneous green crns," *IEEE Transactions on Cognitive Communications and Networking (under revision)*.

[20] S. Chaudhari, J. Lunden, V. Koivunen, and H. V. Poor, "Cooperative sensing with imperfect reporting channels: Hard decisions or soft decisions?" *IEEE Transactions on Signal Processing*, vol. 60, no. 1, pp. 18–28, 2012.

[21] E. Axell *et al.*, "Spectrum sensing for cognitive radio: State-of-the-art and recent advances," *IEEE Signal Processing Magazine*, vol. 29, no. 3, pp. 101–116, May 2012.

[22] A. Celik and A. E. Kamal, "More spectrum for less energy: Green cooperative sensing scheduling in crns," in *proc. IEEE International Conference on Communications (ICC)*, 2015.

[23] M. Fernandez and S. Williams, "Closed-form expression for the Poisson-binomial probability density function," *IEEE Transactions on Aerospace and Electronic Systems*, vol. 46, no. 2, pp. 803–817, Apr. 2010.

[24] Q. Zhao *et al.*, "On myopic sensing for multi-channel opportunistic access: structure, optimality, and performance," *IEEE Transactions on Wireless Communications*, vol. 7, no. 12, pp. 5431–5440, 2008.

[25] S. Boyd and L. Vandenberghe, *Convex optimization*. Cambridge university press, 2004.